

Five years of BRITE-Constellation photometry of the luminous blue variable P Cygni: properties of the stochastic low-frequency variability[★]

Ashley Elliott,¹ Noel D. Richardson,¹ Herbert Pablo,² Anthony F. J. Moffat,³ Dominic M. Bowman,⁴ Nour Ibrahim,⁵ Gerald Handler,⁶ Catherine Lovekin,⁷ Adam Popowicz,⁸ Nicole St-Louis,³ Gregg A. Wade,⁹ and Konstanze Zwintz¹⁰

¹Department of Physics and Astronomy, Embry-Riddle Aeronautical University, 3700 Willow Creek Rd, Prescott, AZ, 86301, USA

²American Association of Variable Star Observers, 49 Bay State Road, Cambridge, MA 02138, USA

³Centre de Recherche en Astrophysique du Québec, Département de physique, Université de Montréal, Complexe des Sciences, Montréal, QC H2V 0B3, Canada

⁴Institute of Astronomy, KU Leuven, Celestijnenlaan 200D, 3001 Leuven, Belgium

⁵Department of Astronomy, University of Michigan, 1085 S. University, Ann Arbor, MI 48109, USA

⁶Nicolaus Copernicus Astronomical Center, Polish Academy of Sciences, Bartycka 18, PL-00-716 Warsaw, Poland

⁷Physics Department, Mount Allison University, Sackville, NB, Canada

⁸Department of Electronics, Electrical Engineering and Microelectronics, Silesian University of Technology, Akademicka 16, 44-100 Gilwice, Poland

⁹Department of Physics and Space Science, Royal Military College of Canada, PO Box 17000, Station Forces, Kingston, ON, Canada K7K 7B4

¹⁰University of Innsbruck, Institute for Astro- and Particle Physics, Technikerstrasse 25/8, A-6020 Innsbruck, Austria

Accepted XXX. Received YYY; in original form ZZZ

ABSTRACT

Luminous Blue Variables (LBVs) are massive stars that are likely to be a transitional phase between O stars and hydrogen-free classical Wolf-Rayet stars. The variability of these stars has been an area of study for both professional and amateur astronomers for more than a century. In this paper, we present five years of precision photometry of the classical LBV P Cygni taken with the BRITE-Constellation nanosatellites. We have analyzed these data with Fourier analysis to search for periodicities that could elucidate the drivers of variability for these stars. These data show some long-timescale variability over the course of all six calendar years of observations, but the frequencies needed to reproduce the individual light curves are not consistent from one year to the next. These results likely show that there is no periodic phenomenon present for P Cygni, meaning that the variability is largely stochastic. We interpret the data as being caused by internal gravity waves similar to those seen in other massive stars, with P Cygni exhibiting a larger amplitude and lower characteristic frequency than the main-sequence or blue supergiant stars previously studied. These results show evidence that LBVs may be an extrapolation of the blue supergiants, which have previously been shown to be an extension of main-sequence stars in the context of the stochastic low-frequency photometric variability.

Key words: stars: massive – stars: mass-loss – stars: variables: S Doradus – stars: winds, outflows

1 INTRODUCTION

Luminous blue variable stars (LBVs) are massive, post main-sequence stars that have strong winds and exhibit multiple types of variability, with the time-scales of the variations ranging from days to centuries. These stars are important for understanding the evolution of stellar feedback for future star formation, despite there only being ~60 known LBVs or candidate LBVs in the current census of the stars (Richardson & Mehner 2018). LBVs have been observed to have their

brightness increase and exhibit supernova-like changes in their light-curves, at which time the star expels upwards of a few solar masses of material in a short time frame (e.g., Humphreys & Davidson 1994). The most famous of these eruptive events are those associated with the Galactic LBVs η Carinae and P Cygni. van Genderen (2001) describes the properties a star must meet in order to be considered an LBV, or S Dor variable. These include visible ejecta, spectroscopic characteristics that indicate the unique characteristics of an LBV, and photometric variability that has a time scale of anywhere between days and even centuries. They also define the S Doradus phase (SD-phase) to be the time periods when the star exhibits a cyclic pattern of brightening in the optical and apparent changes in the stellar wind properties, while the star maintains a roughly constant bolometric luminosity (e.g., Humphreys & Davidson 1994).

The main cause of the SD-phases, according to van Genderen (2001), are the radius and the temperature variations of the star. These phases have roughly constant bolometric luminosity but the

[★] Based on data collected by the BRITE Constellation satellite mission, designed, built, launched, operated and supported by the Austrian Research Promotion Agency (FFG), the University of Vienna, the Technical University of Graz, the University of Innsbruck, the Canadian Space Agency (CSA), the University of Toronto Institute for Aerospace Studies (UTIAS), the Foundation for Polish Science & Technology (FNiTP MNiSW), and National Science Centre (NCN).

temperature and radius vary throughout these phases. The effective temperatures of these stars tend to be in the range of 15,000 to 30,000 K. There are two main types of an SD-phase, one on a timescale of years and one on a timescale of decades, referred to as the short (S) SD-phase and long (L) SD-phase, respectively. During the SD-phases, the observed magnitude of an LBV varies (up to $\sim 1\text{--}2$ mag) over the span of several years or decades, due to the underlying changes in the effective temperature and radius. During the SD-phase, LBVs appear to change between a hot visual minimum state to a cool visual maximum state, during which the stars maintain an almost constant bolometric luminosity near the Eddington limit (Humphreys & Davidson 1994).

Despite several models having been developed to explain the LBV phenomenon in the context of single star evolution (Grassitelli et al. 2021), the causes of the LBV phenomenon and the evolutionary status of these objects are both still debated, especially given the strong evidence that binary evolution dominates the evolution of massive stars (Sana et al. 2012). In recent years, Smith & Tombleson (2015) suggested that the LBVs are actually the result of binary evolution. This hypothesis relied on LBVs being relatively isolated compared to other massive stars such as O stars and WR stars. Humphreys et al. (2016) and Aadland et al. (2018) reexamined the population of LBVs and found that the spatial distribution of other massive, hot stars was indeed similar to that of LBVs, while Smith (2019) found instead that the stars are more isolated than typical O stars. Binary evolution may still allow us to explain several phenomena related to the eruptions and LBV properties. For example, the eruption of η Carinae could be explained by a merger in a triple star system that resulted in the present-day eccentric binary (e.g., Hirai et al. 2021). Furthermore, the LBVs HR Carinae and AG Carinae have been shown to be rapid rotators in certain portions of the SD-phases, namely when the star is hottest and has the smallest radius, which could be a result of previous binary mergers or mass transfer (Groh et al. 2009b,a). Also, some evidence exists for rapid rotation of η Carinae (Groh et al. 2012).

One of the classical LBVs with a long observational record is P Cygni. In August 1600, it made its first documented “appearance” in the sky, reaching third magnitude and then fading below naked-eye visibility. This was the first eruption of P Cygni, discovered by Willem Janszoon Blaeu, a former student of Tycho Brahe’s, who recorded the discovery in his celestial globe made in his Amsterdam workshop in 1602. A second eruption was observed in 1654. Since this time, P Cygni has become somewhat stable near fifth magnitude (Humphreys & Davidson 1994) but also showing a gradual brightening of the star occurring over very long time scales. The long-term brightening was most recently measured to be 0.17 ± 0.01 mag century $^{-1}$, similar to other studies of this phenomenon (Richardson et al. 2011).

P Cygni is an ideal test bed for our understanding of LBVs, due to its enhanced brightness and relatively small distance. Spectral modeling with the non-LTE radiative transfer code CMFGEN has revealed that the star has a mass-loss rate of $3.0 \times 10^{-5} M_{\odot} \text{yr}^{-1}$, a terminal wind speed of $v_{\infty} = 185 \text{ km s}^{-1}$, and an observed effective temperature of 18,500 K (Najarro et al. 1997). These spectral models are derived assuming a spherically symmetric wind, which has been tested with multiple observational techniques. With long-baseline optical interferometry with the Naval Precision Optical Interferometer, Balan et al. (2010) found the $H\alpha$ emitting region to be spherically symmetric and stable with about a 10% deviation from observations taken during the time period of 2005–2008. Similarly, Richardson et al. (2013) created the first images of the wind using observations in the H -band with the CHARA interferometer and found that the wind was very close to spherically

symmetric. Richardson et al. (2011) examined the long-term variability properties of the $H\alpha$ profile, which revealed subtle structures in the absorption trough that could be explained under the assumptions of spherical symmetry. Gootkin et al. (2020) examined over a decade of spectropolarimetry to reveal and confirm that P Cygni’s wind produces intrinsic polarization almost certainly from clumping. However, the lack of preferred direction implies that the wind is spherically symmetric on the whole, in agreement with other studies (e.g., Taylor et al. 1991) since changes in the position angle happen much faster than the typical flow time of the stellar wind.

With the brightness and eruptive history of P Cygni, many studies of the star’s variability have been carried out in an attempt to understand the properties and evolutionary status of this object. Photometric studies began in earnest with Percy & Welch (1983), Percy et al. (1988), and de Groot (1990). These studies displayed three major timescales: a short period around 17 days associated with typical α Cygni variability, a ~ 100 day period similar to other known LBVs, and a cycle of years that can be classified as a short SD-phase. These timescales were confirmed by de Groot et al. (2001a). Spectroscopically, the star has been studied most notably by Markova et al. (2001b) and Richardson et al. (2011). Markova et al. (2001b) compared previously noted UBV photometric data and new $H\alpha$ spectroscopy. These photometric data confirm the presence of a slow variation in brightness on a timescale of 7.4 years. The $H\alpha$ equivalent width determinations indicate the presence of a slow component, dubbed the Very-Long Term Component, in the variability of $H\alpha$, and is also a part of the variable SD-phase of the star. In recent years, the star has become a popular object for amateur astronomers to collect simultaneous spectroscopy and photometry, which has led to a possible detection of a 318 d period in the $H\alpha$ profile (Pollmann & Bauer 2012; Pollmann & Vollmann 2013; Pollmann 2016, 2020).

The spherically symmetric wind of this LBV makes the interpretation of its variability simpler to interpret. When combined with P Cygni’s rich observational history and brightness, P Cygni is an ideal star with which to study LBVs. We have analyzed five years of precision photometry from the *Bright Target Explorer*-Constellation nanosatellites (*BRITE*). We present these observations in Section 2, and our Fourier analysis in Section 3. We then discuss these observations in Section 4 and conclude our study in Section 5.

2 OBSERVATIONS

BRITE-Constellation refers to five operational nanosatellites: *BRITE-Austria* (*BAb*), *UniBRITE* (*UBr*), *BRITE-Lem* (*BLb*), *BRITE-Heweliusz* (*BHr*), and *BRITE-Toronto* (*BTr*). The small letter appended to each abbreviation indicating the passband in which each satellite operates (“b” for a blue filter covering 3900–4600Å, and “r” for a red filter covering 5450–6950Å). The satellites are located in low-Earth orbits with orbital periods of the order of 100 min. Each of the $20 \times 20 \times 20 \text{ cm}^3$ *BRITE* nanosatellites is equipped with a 3-cm telescope feeding an uncooled 4008 \times 2672-pixel KAI-11002M CCD, with a large effective unvignetted field of view of $24^{\circ} \times 20^{\circ}$ to fulfil a single purpose: tracking the long-term photometric variability of bright stars ($V \leq 6$) in two passbands, typically over time periods of 2–6 months. Full technical descriptions of the mission were provided by Weiss et al. (2014) and Pablo et al. (2016).

P Cygni was observed during five observation campaigns of *BRITE*. Our data spanned the time period from 2014 to 2019, with no observations made in 2017. For consistency, we are only using the red-filtered data, as the blue data were less consistent and much more sparse. The only *BRITE* satellite used for this study is *BRITE Toronto*.

Year	Start HJD	End HJD	Number of Binned Data Points	Typical Error
2014	2456847.232	2456924.455	657	0.00214
2015	2457184.674	2457340.628	2111	0.00172
2016	2457512.732	2457651.967	1731	0.00193
2018	2458274.668	2458385.975	1170	0.00208
2019	2458648.635	2458788.511	1737	0.00865

Table 1. Properties of the final *BRITE-Toronto* light curves.

There were some data taken with the blue-filtered satellites, which were of much lower precision due to the efficiency of the system and narrower bandpass. Furthermore, the data taken with *UniBRITE* was found to be of too low precision in comparison to the data from the *BRITE Toronto* satellite. The data were processed in the standard manner for the *BRITE* satellites and binned to orbital means as no variability has been observed for the star with time-scales faster than 100 minutes in the past (Pablo et al. 2016; Popowicz 2016; Popowicz et al. 2017). These reduced photometric data were examined and we found large jumps in relative fluxes between different portions of the light curve that were reduced separately during the pipeline process in order to mitigate problems with dark current (e.g., Popowicz 2018; Popowicz & Farah 2020). To rectify this problem, we calculated linear fits near the ends of each data set in order to minimize the gap between the setups for each data set. Once a linear fit was found, the y-intercepts were subtracted from one another and that value was added to the flux data for one set so that these data were overlapping, and repeated for each small time string. This process was compared to the AAVSO V-band light curves to ensure the light curves provided consistent variability with the observational record. The AAVSO light curve suffers from much lower precision than the *BRITE* light curves, so if the AAVSO data were too sparse in the regions where we performed a linear fit, we would compare the average flux levels of the adjacent time-series to ensure that the derived fit was reasonable. This is illustrated in Fig. 1, with a comparative light curve of the AAVSO data and the *BRITE* data shown in the supplementary material. In general, this process is well-supported with the comparison to the AAVSO fluxes (e.g., Fig. 1 and Fig. A1). There may be some additional long-period ($t \sim 3 - 4$ yr) noise added in our final year of data from *BRITE*, but the noise levels on our data are also the highest in these data.

Once the data were reduced into one continuous data set that showed a consistent light curve, we used AAVSO photometry to calculate average magnitudes for each year. This average magnitude was then converted into flux and subtracted from each year in order to center the data around 0. Given the large flux from the wind, especially in the $H\alpha$ line, we show a plot with a typical spectrum of P Cygni from the ARAS database¹ in Fig. 2 with the *BRITE* filter response overplotted for understanding our measurements.

3 FOURIER ANALYSIS

To find significant periodicities in the *BRITE* data, we performed a Fourier analysis. To begin, we examined our complete light curve (Fig. 3), and then calculated the Fourier spectrum with the `Period04` software available from Lenz & Breger (2005). With this analysis, we found one peak at a frequency of 0.001045 d^{-1} , corresponding to a period of 956.8 d (2.65 years). We utilized the methods described by Pablo et al. (2017) to determine the noise limit of these data through

¹ http://www.astrosurf.com/aras/Aras_DataBase/LBV/PCyg.htm

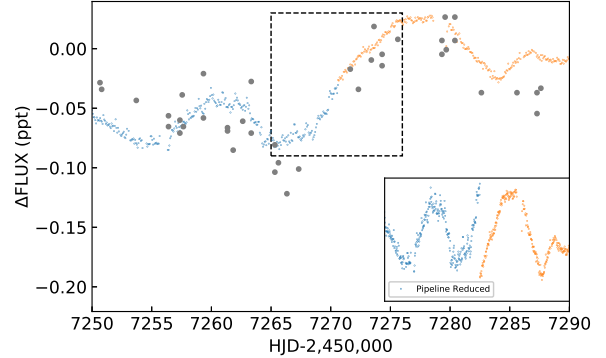


Figure 1. An example of the merging of two subsets of data from 2015 that were combined to create a more continuous data set. A linear fit was done to both the blue and orange points within the central box with dashed lines, and then they are shifted to match. The inset panel on the bottom right shows the pipeline-reduced and binned light curve at the same time frame, highlighting the need for the changes. The final reduced data were compared to the AAVSO V-band light curve to ensure consistency, which is shown as grey points after being converted to flux here..

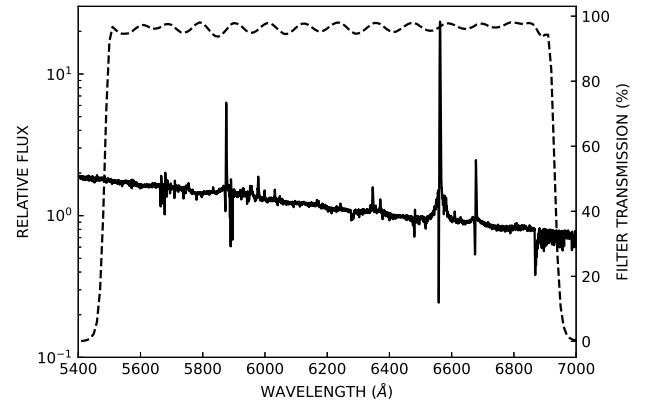


Figure 2. A typical spectrum of P Cygni, downloaded from the ARAS database, with the red *BRITE* filter response overplotted.

a false alarm probability and then calculate a signal-to-noise ratio based on the strength of the peak divided by the noise level at that frequency. We also calculate a $\sigma(O - C)$ as the standard deviation of the quantity of the difference between the observed and calculated points, the $(O - C)$ curve, after that fit. If adding additional terms from the Fourier analysis does not alter the value of $\sigma(O - C)$, then additional terms can be rejected. Our full analysis of the light curve shows that the 956.8 d “period” was marginally detected with a signal-to-noise ratio of 1.9 and an amplitude of 63.4 parts per thousand (ppt),

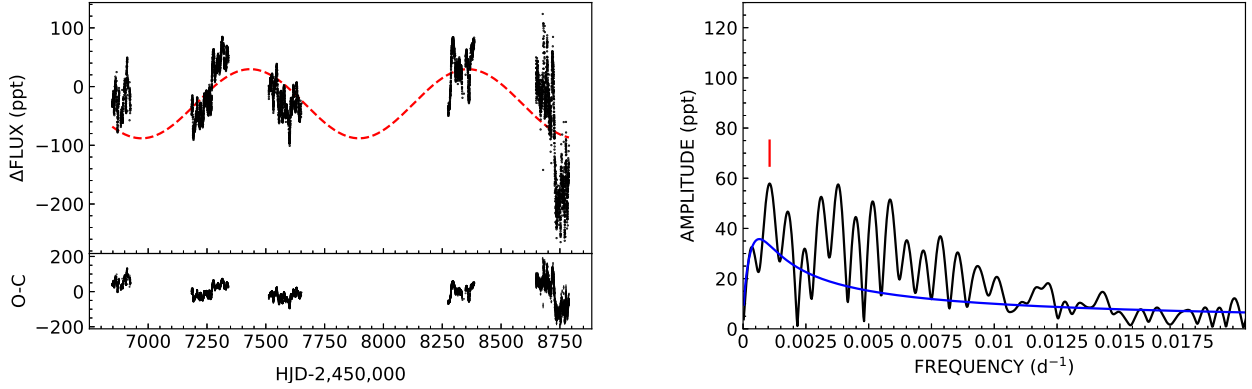


Figure 3. In the left plot, we show all available *BRITE* fluxes used in our analysis, after subtracting off the global mean, with units of parts per thousand (ppt), with our calculated Fourier spectrum on the right. The frequency indicated in red on the Fourier amplitude spectrum indicates the strongest frequency from the Fourier analysis, with the blue curve representing the noise in this spectrum. The bottom panel of the photometric light curve shows the difference between the observed and calculated light curve for these data.

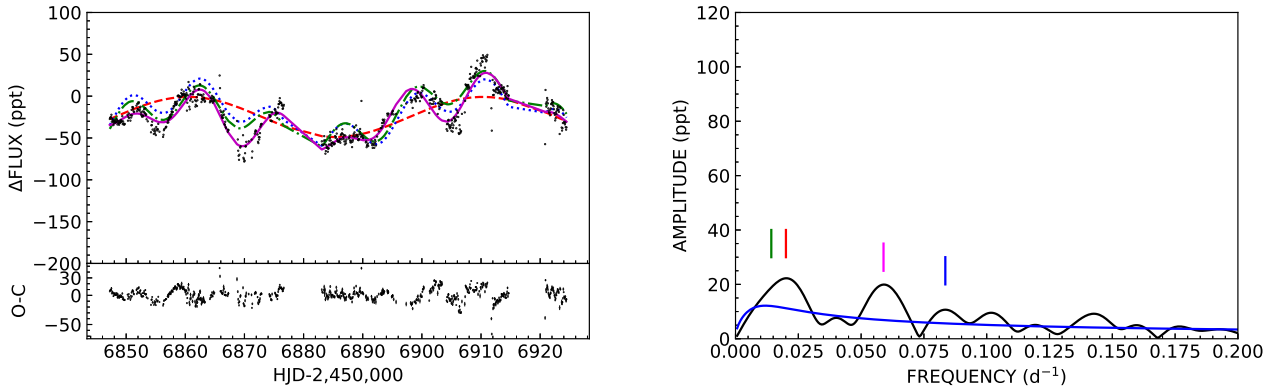


Figure 4. The *BRITE* flux, after subtracting off the global mean, with units of parts per thousand (ppt) (left) and the Fourier amplitude spectrum (right) for the 2014 data from *BRITE*. Each peak used in our analysis is highlighted with a different color in the Fourier spectrum, and then the fit is overplotted on the photometry with the corresponding color for that term and all previous terms. The final four-frequency fit is then used to calculate the ($O - C$) that is shown on the bottom panel of the photometry. The term numbers from Table 2 are given by: Term 1 is shown in the red dashed line, Term 2 is shown in the dotted blue line, Term 3 is shown in the dashed and dotted green line, and Term 4 is shown as the solid pink line, where each term includes the previous ones in the fit.

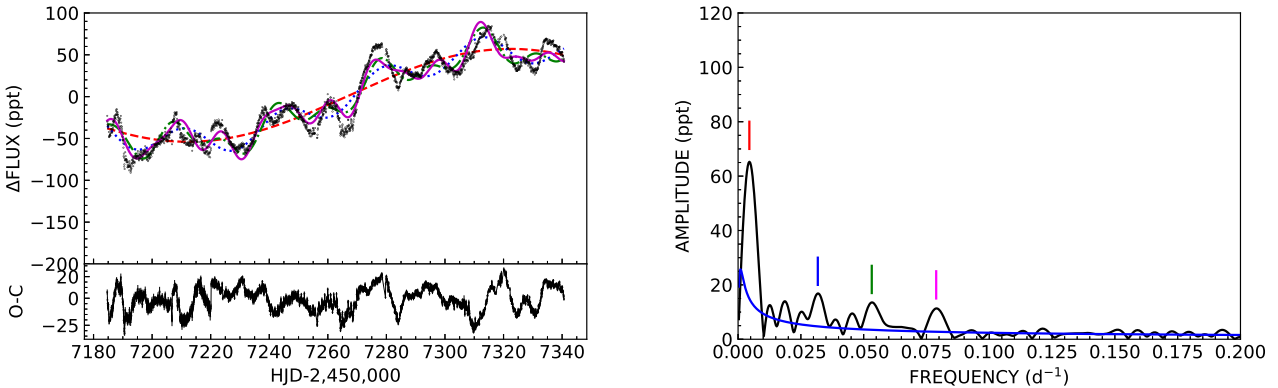


Figure 5. The *BRITE* flux, after subtracting off the global mean, with units of parts per thousand (ppt) (left) and the Fourier amplitude spectrum (right) for the 2015 data from *BRITE*, format as in Fig. 4.

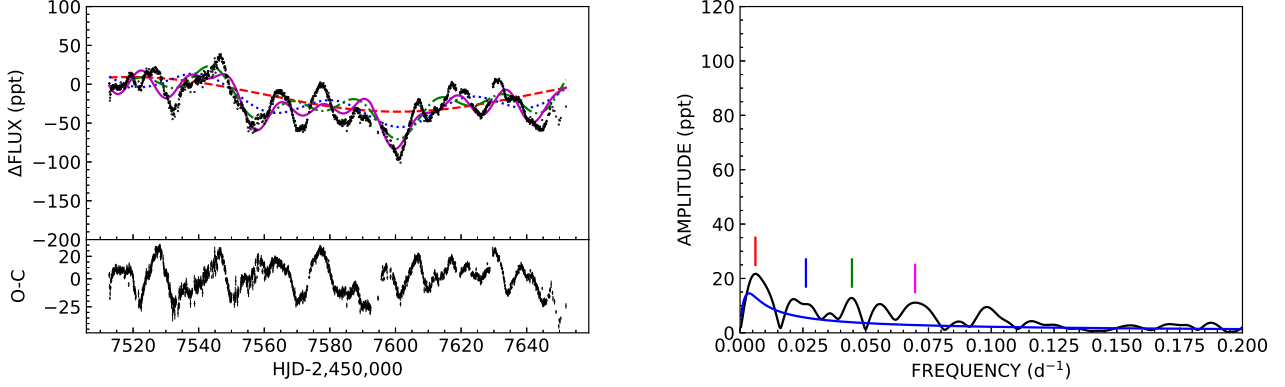


Figure 6. The *BRITE* flux, after subtracting off the global mean, with units of parts per thousand (ppt) (left) and the Fourier amplitude spectrum (right) for the 2016 data from *BRITE*, format as in Fig. 4.

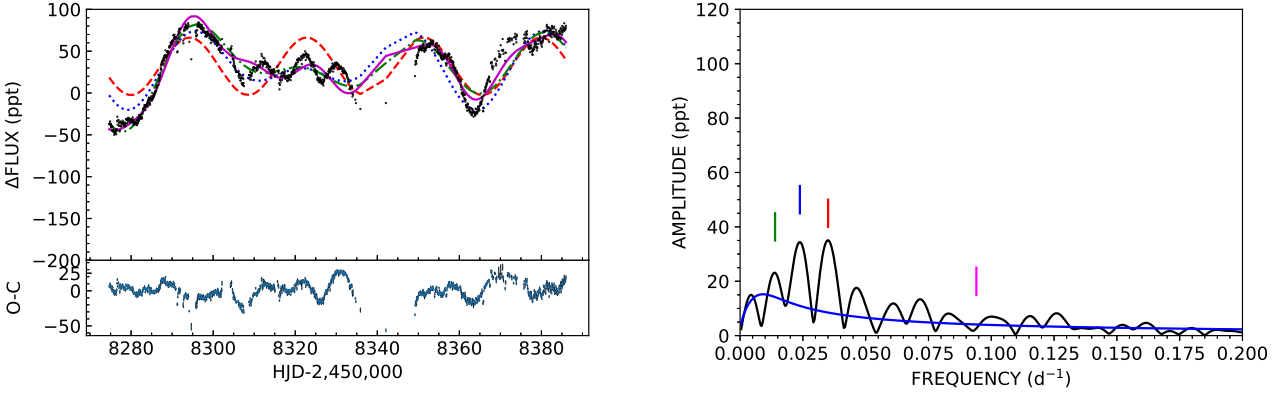


Figure 7. The *BRITE* flux, after subtracting off the global mean, with units of parts per thousand (ppt) (left) and the Fourier amplitude spectrum (right) for the 2018 data from *BRITE*, format as in Fig. 4.

as shown in Fig. 3. No additional frequencies significantly improved the fit to the full *BRITE* data set.

Next we analysed individual observational campaigns of *BRITE* observations. For each season of *BRITE* photometry, we performed a similar analysis using the *Period04* software and found four frequencies that we include in our analysis. These fits are shown in Figures 4–8. For each season, we present in Table 2 the term number i that we use in the equation

$$F = ZP + \sum_{i=1}^4 A_i \sin(2\pi(f_i t + \phi_i))$$

to reproduce the light curve, where ZP is a zero point of the data, f_i is the i^{th} frequency and ϕ_i is a phase. These are all relative to time t , which was calculated to be relative to the heliocentric Julian Date (-2,450,000). Each figure for the datasets (Fig. 4–8) shows the addition of the individual terms as additional sine waves with the different colors of the associated sine waves. Each iteration was then improved upon so that some peaks we derive do not appear directly in the original Fourier transform (e.g., Fig. 7), but this is in part due to the low signal-to-noise of these peaks.

The signal-to-noise of the derived peaks is typically low, with a S/N usually being ≤ 2 . Baran et al. (2015) showed that for the more precise, higher cadence *K2* data, a S/N of 5 is preferred as to not over

interpret the light curve with respect to pulsations. We also measure a goodness of fit with a standard deviation of the residuals of the ($O - C$) curve, which we report as $\sigma_{(O-C)}$ in Table 2.

4 DISCUSSION

We have collected the first high-precision and high-cadence light curve of a luminous blue variable. This has allowed us to explore the light curve with Fourier analysis in an attempt to discover periodicities that are intrinsic to the star.

Our Fourier analysis presented in Section 3, did not produce any frequencies that were significant with a S/N of 4 or higher based on the methods described by Pablo et al. (2017). Since the light curve of this typical luminous blue variable is most certainly variable compared to the errors of the data, we must therefore look for alternate explanations of the variability.

In a recent spectroscopic analysis, Pollmann (2020) reported a periodic behavior of the $H\alpha$ equivalent width for *P Cygni*, and reported a 318-d period for the time period covering 2005–2019. If confirmed, a strict periodicity would be extremely interesting as no other study has found a strict periodicity for *P Cygni*. In contrast, Richardson et al. (2018) found that there are two periods in the *BRITE* light curves of η Carinae over two years, which they were able to compare to the

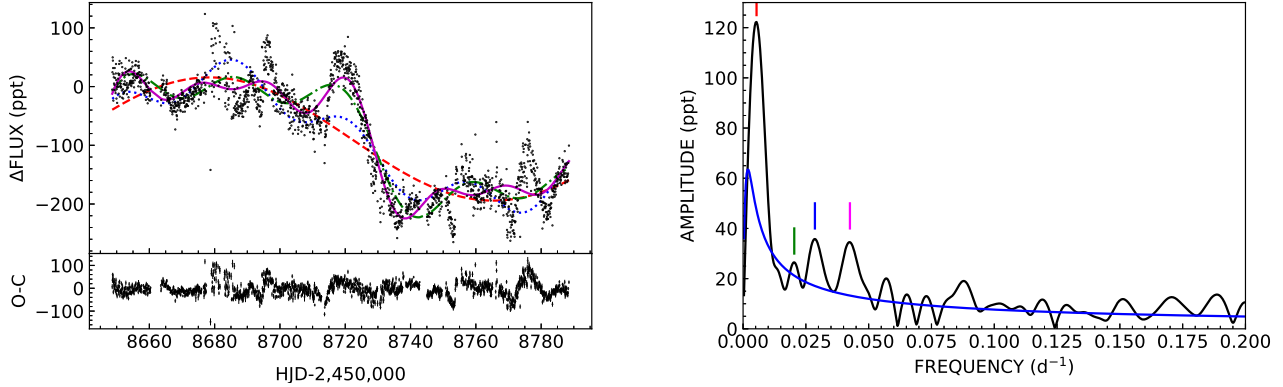


Figure 8. The *BRITE* flux, after subtracting off the global mean, with units of parts per thousand (ppt) (left) and the Fourier amplitude spectrum (right) for the 2019 data from *BRITE*, format as in Fig. 4.

Term number	Frequency (d^{-1})	Amplitude (ppt)	Phase	$\sigma_{(O-C)}$ (ppt)	S/N
2014, ZP: -0.02556 ± 0.00043					
1	0.02553 ± 0.00029	14.45 ± 0.77	0.02498 ± 0.067	19.13	1.39
2	0.08469 ± 0.00026	16.89 ± 0.72	0.6762 ± 0.0060	15.15	3.02
3	0.01375 ± 0.00024	19.39 ± 0.66	0.1637 ± 0.0057	13.33	1.60
4	0.05780 ± 0.00029	14.31 ± 0.58	0.7383 ± 0.0070	10.70	2.06
2015, ZP: 0.00019 ± 0.00029					
1	0.00428 ± 0.00004	55.26 ± 0.36	0.7778 ± 0.0012	17.92	3.56
2	0.02966 ± 0.000088	14.51 ± 0.32	0.0844 ± 0.0037	14.78	2.98
3	0.05474 ± 0.00010	12.95 ± 0.35	0.8960 ± 0.0038	12.45	3.78
4	0.07937 ± 0.00016	7.957 ± 0.34	0.5445 ± 0.0062	10.81	2.92
2016, ZP: -0.0125 ± 0.0016					
1	0.00554 ± 0.00062	27.34 ± 1.32	0.2563 ± 0.0028	20.91	2.27
2	0.02482 ± 0.00018	14.99 ± 0.93	0.8460 ± 0.0047	18.15	2.91
3	0.04487 ± 0.00020	13.10 ± 0.69	0.4488 ± 0.0056	15.28	2.98
4	0.07183 ± 0.00030	11.73 ± 4.14	0.9263 ± 0.0062	12.98	3.86
2018, ZP: 0.03146 ± 0.00042					
1	0.03246 ± 0.0062	41.70 ± 1.32	0.2613 ± 0.0034	22.81	4.66
2	0.02675 ± 0.0002	41.75 ± 0.92	0.4738 ± 0.0032	15.61	4.09
3	0.01989 ± 0.0002	18.62 ± 0.69	0.1041 ± 0.0040	12.45	1.53
4	0.09407 ± 0.0030	7.766 ± 4.14	0.4059 ± 0.021	11.19	1.90
2019, ZP: -0.01247 ± 0.0016					
1	0.00631 ± 0.0062	109.3 ± 1.32	0.06254 ± 0.0017	47.85	2.55
2	0.02934 ± 0.00018	35.80 ± 0.92	0.9423 ± 0.0049	42.57	2.13
3	0.01784 ± 0.00020	35.76 ± 0.69	0.3644 ± 0.0055	35.22	1.55
4	0.04158 ± 0.00030	23.91 ± 4.14	0.8699 ± 0.0070	31.37	1.94
All Data, ZP: -0.03127 ± 0.00067					
1	0.00105 ± 0.0023	63.43 ± 0.87	0.09368 ± 0.0030	53.12	1.95

Table 2. The resulting coefficients from the Fourier analysis of our data. The phase is relative to the zero-point of the HJD calendar.

tidally excited oscillations that have been seen for many eccentric binaries across the H-R diagram.

P Cygni is not a well-established binary. [Kashi \(2010\)](#) modelled the eruptive light curve as caused by binarity, but the light curve from the time of the eruption is not a well-recorded time-series. The light curve modelled by [Kashi \(2010\)](#) was actually that of [de Groot \(1988\)](#),

which was re-evaluated by [Smith et al. \(2011\)](#) who concluded that the eruptive light curve of P Cygni has a more “typical” appearance of an LBV eruption when we consider the sparsely sampled light curve. [Richardson et al. \(2013\)](#) found no indication of a companion from interferometric observations with a limiting magnitude difference of $\Delta H = 5.3$, while a recent examination of the multiplicity of LBVs

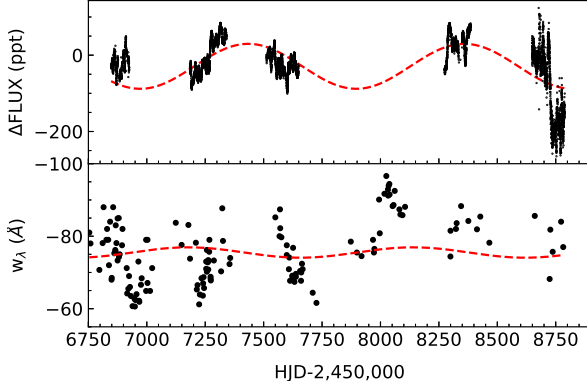


Figure 9. We compare our results on the Fourier analysis of all of the *BRITE* data to the measured $H\alpha$ equivalent widths measured by Pollmann (2020). The 950-d period from our photometric analysis (see Fig. 3) is shown as a dashed red line, and is also forced to fit the $H\alpha$ measurements.

by Mahy et al. (2021) reported a possible companion with $\Delta H = 4.3$, a full magnitude brighter than the limiting magnitude reported by Richardson et al. (2013), although Mahy et al. (2021) searched over a larger field-of-view.

If the 318 d period reported by Pollmann (2020) is confirmed, it could represent a pulsation mode driven by tidal forces, such as that in the massive binary ι Ori (Pablo et al. 2017) or the LBV binary η Car (Richardson et al. 2018). This could also represent a normal pulsation for supergiants (Maeder 1980). However, we cannot photometrically confirm the 318 d period that was reported from the study of $H\alpha$ equivalent widths, although it is possible that the 318 d period shown in Fig. 9 could represent a harmonic of the ~ 950 d period. Unfortunately, the significance of that periodicity in the *BRITE* data is only 2σ above the noise level of the Fourier spectrum (Table 2). We compare these data sets in Fig. 9, but also caution that searching for a 318-d period in our *BRITE* data is difficult owing to the length of the data-sets (~ 150 d) and their being spaced by ~ 0.5 yr apart.

Both Markova et al. (2001a,b) and Richardson et al. (2011) studied the long-term photometric trends in relation to the trends observed with $H\alpha$. These studies all found a positive correlation between the $H\alpha$ equivalent widths and V -band photometry. We calculated the needed amplitude and phase for a period that was the same as our derived photometric period shown in Fig. 3, and show these in Fig. 9.

When comparing the $H\alpha$ measurements over the same time period as the photometry, we found that the two data sets could show similar variability time scales. The raw curves show similar trends, with an increase in flux and equivalent width across the 2015 data set and a decrease in 2016. The 2018 and 2019 $H\alpha$ data sets were too sparse to see similar trends in the data. However, the times of the maxima derived from this analysis are different for both data sets. The data-sets are likely correlated, but the gap in the *BRITE* observations in 2017 and the sparse ground-based observations of $H\alpha$ will prevent a firm analysis of this correlation, and any photometric periodicity lies below a S/N of 4 that is typical for confirmation of periodicities.

4.1 Properties of the stochastic low-frequency variability

Recent advances in astronomical time-series have revolutionized our understanding of massive star asteroseismology (see Bowman 2020, for a recent review). With the advent of all-sky surveys searching for planet transits, time-series photometry of massive stars has become

Time scale	Interpretation or Discovery type	Reference
~ 7.3 yr	SD-phase	1
1700 d	$H\alpha$ discrete absorption component recurrence time	2
~ 4 yr	SD-phase radial pulsations	3, 4, 5, 6
	gravity wave, but non-radial pulsations	3, 5
	gravity wave, but non-radial pulsations	7
$\sim 900 - 1000$ d	long-term photometry	This work
	gravity waves, sub-surface convection	
~ 700 d	$H\alpha$ discrete absorption component progression time	2
~ 500 d	pressure wave	7
318.3 d	$H\alpha$ equivalent width	8
~ 175 d	pressure wave	7
~ 100 d	pressure wave or other type of oscillation	4, 5, 7
17.3 d	α Cyg osc.	4, 5

Table 3. Previous periods and timescales reported for P Cygni with their interpretation and discovery method. References are 1: Markova et al. (2000), 2: Richardson et al. (2011), 3: Markova et al. (2001a), 4: de Groot et al. (2001a), 5: de Groot et al. (2001b), 6: Markova et al. (2001b), 7: de Jager (2001), and 8: Pollmann (2020).

a useful tool in studying these types of stars, and two general explanations have been used to describe the typical properties of the Fourier transforms for massive stars, namely internal gravity waves (Rogers et al. 2013; Edelmann et al. 2019; Horst et al. 2020) and sub-surface convection (Lecoanet et al. 2019; Cantiello et al. 2021). P Cygni is a well-established LBV, so the long time-series of *BRITE* photometry can be considered a first step towards understanding the driving mechanisms for the long (i.e. ≥ 100 d) and short time-scale (i.e. \lesssim d) variability of luminous blue variables. We have compiled a table of reported time-scales and “periods” for P Cygni in Table 3, along with the interpretation or discovery type of these variations.

The time-scales in Table 3 show P Cygni is known to be variable with periods between 17 d and several years. These have been interpreted as α Cygni-like oscillations for the shortest period oscillations (e.g., de Groot et al. 2001b), consistent with the ideas that the luminous blue variables are extreme versions of normal luminous supergiants. In Figures 4–8, the light curves of P Cygni throughout the *BRITE* campaign are shown. Short-term variations are certainly seen, but rarely is it similar to a 17-d timescale, and that particular period is never required to fit the light curves in Figs. 4–8.

The Fourier transform of the *BRITE* data shows that the variability extends over a broad frequency range, and dominated by longer periods. We used the methods of Bowman et al. (2019b,a, 2020) to fit the white noise and stochastic low-frequency variability components of the Fourier transform with the equation

$$\alpha(\nu) = \frac{\alpha_0}{1 + \left(\frac{\nu}{\nu_{\text{char}}}\right)^\gamma} + C_w.$$

In this equation, α_0 represents the amplitude at a frequency of zero, γ is the logarithmic amplitude gradient, ν_{char} is the characteristic frequency, which is the inverse of the characteristic timescale, τ , of stochastic variability present in the light curve such that $\nu_{\text{char}} = (2\pi\tau)^{-1}$, and C_w is a frequency-independent (white) noise term (Blomme et al. 2011; Bowman et al. 2019b). To fit the equation and derive errors, we utilize the python package emcee (Foreman-Mackey et al. 2013) and derive the terms of $\alpha_0 = 12.8 \pm 0.2$ parts per thousand in fractional flux, $\nu_{\text{char}} = 0.033 \pm 0.001 \text{ d}^{-1}$, $\gamma = 1.04 \pm 0.01$, and $C_w = 0.288 \pm 0.004$ parts per thousand in

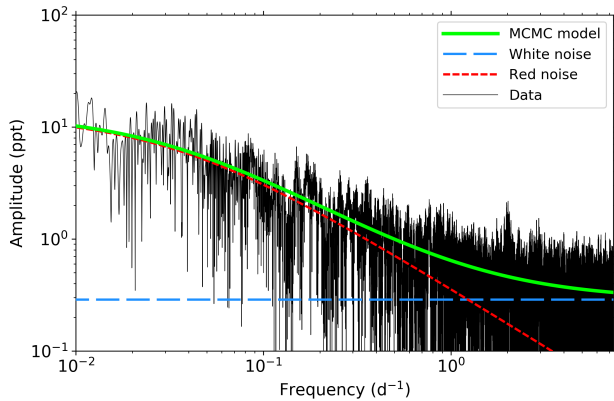


Figure 10. The white- and red-noise fit to the Fourier transform of the *BRITE* data. The model is described in the text.

fractional flux. While we did not fit each individual observational campaign in this same manner, we note that the Fourier analyses of these data sets, shown in Figs. 4–8, all have their “peaks” at levels close to the false-alarm probability noise level, with no periodicity seen with a $S/N \gtrsim 4$. Given the small value of ν_{char} , we note that individual data sets may not be of sufficient duration to fit this for every year of data. The resultant fit of the Fourier transform of the *BRITE* data up to the Nyquist frequency is shown in Fig. 10, which shows that significant variability above the white noise level extends up to $\nu \approx 1 \text{ d}^{-1}$.

The results of Bowman et al. (2019a, 2020) have been used to interpret the variability of *K2* and *TESS* light curves of massive stars as the result of internal gravity waves. Their sample was composed primarily of O and B stars on or near the main sequence. A comparison to the H-R diagram in Bowman et al. (2020, their Fig. 2), we can see that while the effective temperatures of their sample are similar to that of LBVs, most of the stars they analyzed have a luminosity an order of magnitude smaller than P Cygni ($\log L/L_{\odot} = 5.85$; $\log T/K = 4.28$; Najjarro et al. 1997). Therefore, given that Bowman et al. (2020) focused on a sample of main sequence stars using *TESS* data, a direct quantitative comparison with our analysis of P Cygni using *BRITE* data is not possible. Yet, the trends in the fits shown in Bowman et al. (2020) shows that the characteristic frequency, ν_{char} , decreases with increasing luminosity and decreasing temperature, while the amplitude, α_0 , increases with increasing luminosity and decreasing temperature. P Cygni, representing a star with a luminosity an order of magnitude higher than these other blue supergiants fits this trend with a characteristic frequency almost an order of magnitude lower and an amplitude an order of magnitude higher than the stars in the sample of Bowman et al. (2020).

Richardson et al. (2011) found that there was no preferred period or timescale in a long 24-year time-series of either spectroscopic measurements or photometry. Their Fourier analysis showed an increase in power with lower frequency, with a shape similar to that shown in Fig. 10. The nature of these variations and timescales show that the star is not a stable pulsator, but does have stochastic low-frequency variability. In many ways, P Cygni seems to behave similarly to the OB stars analyzed by Bowman et al. (2020). In addition to internal gravity waves as a dominant driver of the stochastic low-frequency variability, sub-surface convection could also be responsible. However, the properties of convection and its observational consequences in terms of predicting the time scales of stochastic low-frequency

variability in light curves within the parameter space of P Cygni have yet to be fully explored both theoretically and using numerical simulations (e.g., Jiang et al. 2015). Furthermore, as stars leave the main sequence, stochastic low-frequency variability caused by stellar winds is also expected to become more important, especially in more evolved stars Aerts et al. (e.g., 2018); Krtićka & Feldmeier (e.g., 2021). Our observational study will help guide future theoretical studies of these phenomena. With the *TESS* mission regularly observing the Large Magellanic Cloud, a larger sample of LBVs may be able to be fit similarly in the future for studying the driving mechanisms of these stars as a population.

5 CONCLUSIONS

In this paper, we have studied the luminous blue variable P Cygni with a long-time series of precision photometry collected with the *BRITE-Constellation* of nanosatellites. We have found some interesting results with these data:

- The analysis of the *BRITE* data on P Cygni indicates that the main driver of the variability of this luminous blue variables is similar in morphology in the Fourier spectrum as internal gravity waves seen in main sequence OB stars (Bowman et al. 2020) and stellar winds in evolved stars (Krtićka & Feldmeier 2021). Since no single frequency is persistent across these data sets, the variability is stochastic and not strictly periodic, as has been discussed in past studies.
- Each season of *BRITE* data could be modelled with four frequencies, but these frequencies are not of high significance.
- There is some evidence of a correlation between $H\alpha$ variations and the flux as measured by *BRITE* (Fig. 9).
- There is no single frequency that is persistent in all of these data, and the previously reported ~ 17 day period seen in many datasets (e.g., de Groot et al. 2001b) is not seen in these photometric data at any time. Unlike the massive LBV binary η Car, this lack of persistent period may be an indication that this LBV is a single star showing only stochastic variability, unlike the tidally excited oscillations seen in η Carinae.

ACKNOWLEDGEMENTS

We thank the anonymous referee for comments that improved the presentation of this paper. We acknowledge with thanks the variable star observations from the AAVSO International Database contributed by observers worldwide and used in this research, and in particular the necessary reductions of the *BRITE* photometry. We also acknowledge Ernst Pollmann for making the $H\alpha$ measurements available to us. Adam Popowicz was responsible for image processing and automation of photometric routines for the data registered by *BRITE*-nanosatellite constellation and was supported by grants: 02/140/RGJ21/0012 (SUTO Rector’s grant) and BK-225/RAu-11/2021 (Statutory Activities Grant). AFJM is grateful for financial assistance from NSERC (Canada). GH thanks the Polish National Center for Science (NCN) for support through grant 2015/18/A/ST9/00578. NSL wishes to thank the Natural Sciences and Engineering Council (NSERC) of Canada for financial support. DMB gratefully acknowledges a senior postdoctoral fellowship from the Research Foundation Flanders (FWO) with grant agreement no. 1286521N. GAW acknowledges Discovery Grant support from the Natural Sciences and Engineering Council (NSERC) of Canada.

DATA AVAILABILITY

The raw *BRITE* data are available on the *BRITE* Public archive.² The AAVSO photometry used in the reductions are available at the AAVSO database³. Our reduced light curve is available as a machine-readable table with this publication.

REFERENCES

- Aadland E., Massey P., Neugent K. F., Drout M. R., 2018, *AJ*, **156**, 294
Aerts C., et al., 2018, *MNRAS*, **476**, 1234
Balan A., Tycner C., Zavala R. T., Benson J. A., Hutter D. J., Templeton M., 2010, *AJ*, **139**, 2269
Baran A. S., Koen C., Pokrzywka B., 2015, *MNRAS*, **448**, L16
Blomme R., et al., 2011, *A&A*, **533**, A4
Bowman D. M., 2020, *Frontiers in Astronomy and Space Sciences*, **7**, 70
Bowman D. M., et al., 2019a, *Nature Astronomy*, **3**, 760
Bowman D. M., et al., 2019b, *A&A*, **621**, A135
Bowman D. M., Burssens S., Simón-Díaz S., Edelmann P. V. F., Rogers T. M., Horst L., Röpke F. K., Aerts C., 2020, *A&A*, **640**, A36
Cantiello M., Lecoanet D., Jermyn A. S., Grassitelli L., 2021, *ApJ*, **915**, 112
Edelmann P. V. F., Ratnasingham R. P., Pedersen M. G., Bowman D. M., Prat V., Rogers T. M., 2019, *ApJ*, **876**, 4
Foreman-Mackey D., Hogg D. W., Lang D., Goodman J., 2013, *PASP*, **125**, 306
Gootkin K., et al., 2020, *ApJ*, **900**, 162
Grassitelli L., Langer N., Mackey J., Gräfener G., Grin N. J., Sander A. A. C., Vink J. S., 2021, *A&A*, **647**, A99
Groh J. H., Hillier D. J., Damineli A., Whitelock P. A., Marang F., Rossi C., 2009a, *ApJ*, **698**, 1698
Groh J. H., et al., 2009b, *ApJ*, **705**, L25
Groh J. H., Madura T. I., Hillier D. J., Kruij C. J. H., Weigelt G., 2012, *ApJ*, **759**, L2
Hirai R., Podsiadlowski P., Owocki S. P., Schneider F. R. N., Smith N., 2021, *MNRAS*, **503**, 4276
Horst L., Edelmann P. V. F., Andrásy R., Röpke F. K., Bowman D. M., Aerts C., Ratnasingham R. P., 2020, *A&A*, **641**, A18
Humphreys R. M., Davidson K., 1994, *PASP*, **106**, 1025
Humphreys R. M., Weis K., Davidson K., Gordon M. S., 2016, *ApJ*, **825**, 64
Jiang Y.-F., Cantiello M., Bildsten L., Quataert E., Blaes O., 2015, *ApJ*, **813**, 74
Kashi A., 2010, *MNRAS*, **405**, 1924
Krtićka J., Feldmeier A., 2021, *A&A*, **648**, A79
Lecoanet D., et al., 2019, *ApJ*, **886**, L15
Lenz P., Breger M., 2005, *Communications in Asteroseismology*, **146**, 53
Maeder A., 1980, *A&A*, **90**, 311
Mahy L., et al., 2021, arXiv e-prints, p. arXiv:2105.12380
Markova N., Morrison N., Kolka I., de Groot M., 2000, in Lamers H., Sagar A., eds, *Astronomical Society of the Pacific Conference Series Vol. 204, Thermal and Ionization Aspects of Flows from Hot Stars*. p. 111
Markova N., Scuderi S., de Groot M., Markov H., Panagia N., 2001a, *A&A*, **366**, 935
Markova N., Morrison N., Kolka I., Markov H., 2001b, *A&A*, **376**, 898
Najarro F., Hillier D. J., Stahl O., 1997, *A&A*, **326**, 1117
Pablo H., et al., 2016, *PASP*, **128**, 125001
Pablo H., et al., 2017, *MNRAS*, **467**, 2494
Percy J. R., Welch D. L., 1983, *PASP*, **95**, 491
Percy J. R., et al., 1988, *A&A*, **191**, 248
Pollmann E., 2016, *BAV Journal*, **006**, 1
Pollmann E., 2020, *Journal of the American Association of Variable Star Observers (JAAVSO)*, **48**, 133
Pollmann E., Bauer T., 2012, *Journal of the American Association of Variable Star Observers (JAAVSO)*, **40**, 894
Pollmann E., Vollmann W., 2013, *Journal of the American Association of Variable Star Observers (JAAVSO)*, **41**, 24
Popowicz A., 2016, in *Astronomical Telescopes + Instrumentation*.
Popowicz A., 2018, *Sensors (Basel, Switzerland)*, **18**
Popowicz A., Farah A., 2020, *Remote. Sens.*, **12**, 3633
Popowicz A., et al., 2017, arXiv: Instrumentation and Methods for Astrophysics
Richardson N. D., Mehner A., 2018, *Research Notes of the American Astronomical Society*, **2**, 121
Richardson N. D., Morrison N. D., Gies D. R., Markova N., Hesselbach E. N., Percy J. R., 2011, *AJ*, **141**, 120
Richardson N. D., et al., 2013, *ApJ*, **769**, 118
Richardson N. D., et al., 2018, *MNRAS*, **475**, 5417
Rogers T. M., Lin D. N. C., McElwaine J. N., Lau H. H. B., 2013, *ApJ*, **772**, 21
Sana H., et al., 2012, *Science*, **337**, 444
Smith N., 2019, *MNRAS*, **489**, 4378
Smith N., Tombleson R., 2015, *MNRAS*, **447**, 598
Smith N., Li W., Silverman J. M., Ganeshalingam M., Filippenko A. V., 2011, *MNRAS*, **415**, 773
Taylor M., Nordsieck K. H., Schulte-Ladbeck R. E., Bjorkman K. S., 1991, *AJ*, **102**, 1197
Weiss W. W., et al., 2014, *PASP*, **126**, 573
de Groot M., 1988, *Irish Astronomical Journal*, **18**, 163
de Groot M., 1990, in Garmy C. D., ed., *Astronomical Society of the Pacific Conference Series Vol. 7, Properties of Hot Luminous Stars*. p. 165
de Groot M., Sterken C., van Genderen A. M., 2001a, in de Groot M., Sterken C., eds, *Astronomical Society of the Pacific Conference Series Vol. 233, P Cygni 2000: 400 Years of Progress*. p. 15
de Groot M., Sterken C., van Genderen A. M., 2001b, *A&A*, **376**, 224
de Jager C., 2001, in de Groot M., Sterken C., eds, *Astronomical Society of the Pacific Conference Series Vol. 233, P Cygni 2000: 400 Years of Progress*. p. 215
van Genderen A. M., 2001, *A&A*, **366**, 508

APPENDIX A: THE FULL BRITE AND AAVSO LIGHT CURVE

This paper has been typeset from a $\text{\TeX}/\text{\LaTeX}$ file prepared by the author.

² <https://brite.camk.edu.pl/pub/index.html>

³ <https://www.aavso.org/>

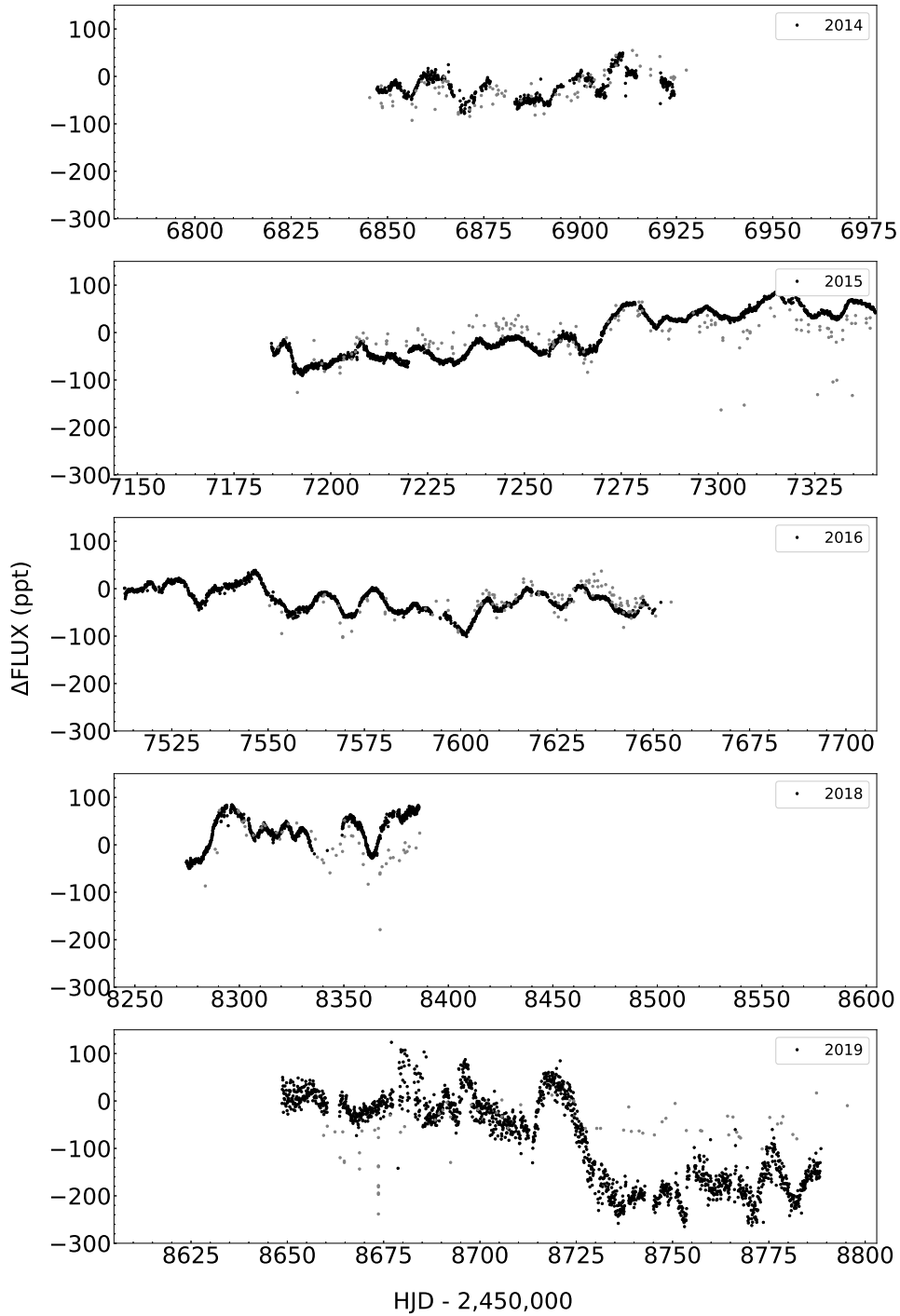


Figure A1. The full BRITe light curve after reductions, with the x-range for each sub-panel representing the time frame of May 15–November 30 of each observing year. In small grey points, we show the AAVSO light curve, converted to differential flux, for comparison.